Cell Membrane Electroporation—Part 1: The Phenomenon

Key words: lipid bilayer, hydrophilic pores, cell plasma membrane, transmembrane voltage, membrane electroporation, transmembrane transport, membrane resealing

T. Kotnik, P. Kramar, G. Pucihar, and D. Miklavčič
Laboratory of Biocybernetics, Faculty of Electrical Engineering, University of Ljubljana, Tržaška 25, SI-1000 Ljubljana, Slovenia

M. Tarek
UMR 7565 CNRS, University of Lorraine, BP 70239, F- 54506 Vandoeuvre-les-Nancy, France

Electrical breakdown of cell membranes (electroporation) can be either reversible of irreversible, each having many applications in medicine and biotechnology. Here, we describe electroporation on the molecular and cellular level.

Introduction

Each biological cell, trillions of which build our bodies, is enveloped by its plasma membrane. Composed largely of a bilayer (double layer) of lipids just two molecules thick (about 5 nm), and behaving partly as a liquid and partly as a gel, the cell plasma membrane nonetheless separates and protects the cell from its surrounding environment very reliably and stably. Embedded within the lipid bilayer, also quite stably, are a number of different proteins, some of which act as channels and pumps, providing a pathway for transporting specific molecules across the membrane. Without these proteins, the membrane would be a largely impenetrable barrier.

Electrically, the cell plasma membrane can be viewed as a thin insulating sheet surrounded on both sides by aqueous electrolyte solutions. When exposed to a sufficiently strong electric field, the membrane will undergo electrical breakdown, which renders it permeable to molecules that are otherwise unable to cross it. The process of rendering the membrane permeable is called *membrane electroporation*. Unlike solid insulators, in which an electrical breakdown generally causes permanent structural change, the membrane, with its lipids behaving as a two-dimensional liquid, can spontaneously return to its pre-breakdown state. If the exposure is sufficiently short and the membrane recovery sufficiently rapid for the cell to remain viable, electroporation is termed *reversible*; otherwise, it is termed *irreversible*.

Since its discovery [1]–[3], electroporation has steadily gained ground as a useful tool in various areas of medicine and biotechnology. Today, reversible electroporation is an established method for introducing chemotherapeutic drugs into tumor cells (*electrochemotherapy*) [4]. It also offers great promise as a technique for gene therapy without the risks caused by viral vectors (*DNA electrotransfer*) [5]. In clinical medicine, irreversible electroporation is being investigated as a method for tissue ablation (*nonthermal electroablation)* [6], whereas in biotechnology, it is useful for extraction of biomolecules [7] and for microbial deactivation, particularly in food preservation [8].

This article, the first in a series of three focusing on electroporation, describes the phenomenon at the molecular level of the lipid bilayer, and then proceeds to the cellular level, explaining how exposure of a cell as a whole to an external electric field results in an inducement of voltage on its plasma membrane, its electroporation, and transport thorough the electroporated membrane. The second article will review the most important and promising applications of electroporation, and the third article will focus on the hardware for electroporation (pulse generators and electrodes) and on the need for standards, safety, and certification.

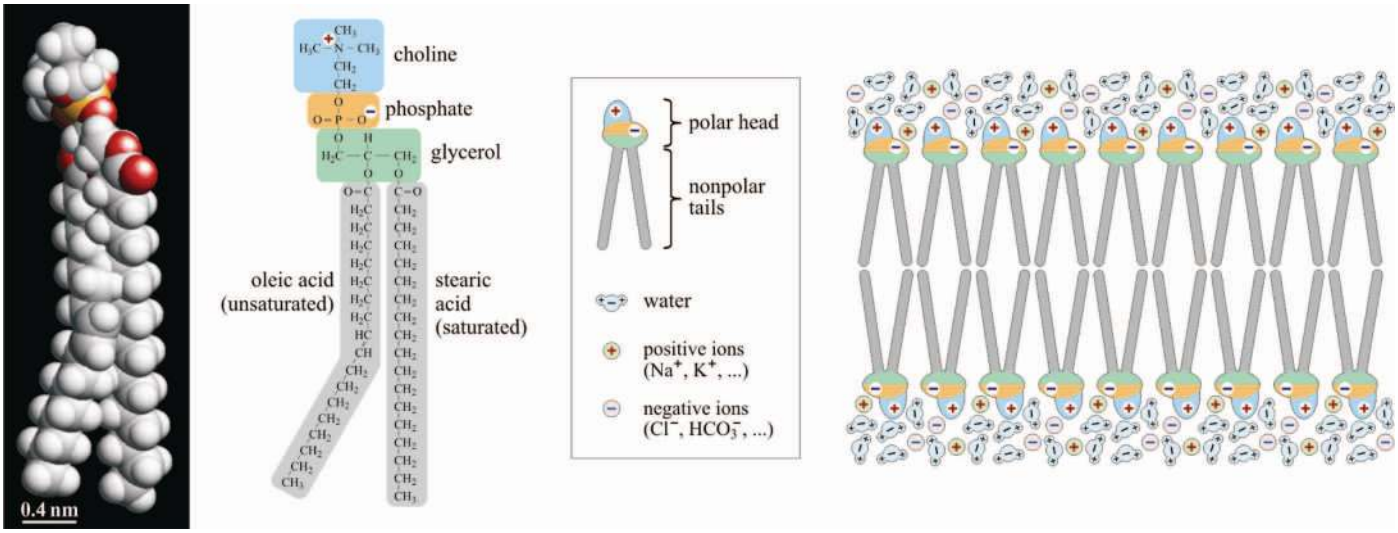

Figure 1. Left: space-filling model and structural formula of the SOPC (1-stearoyl-2-oleoyl-phosphatidylcholine) molecule, a typical membrane lipid. Right: a bilayer of such lipids in an aqueous electrolyte solution.

Lipid Bilayer in an Electric Field

The Lipids, the Bilayer, and the Aqueous Pores

The main molecular constituents of every cell membrane are the lipids. The most abundant are phospholipids (Figure 1), but typical biological membranes also contain glycolipids and cholesterol. Each of these three major lipid classes has a polar (hydrophilic) and a nonpolar (hydrophobic) part. Typically, the polar part is rather compact and the nonpolar part is more elongated, so they are often referred to as the "head" and the "tails" of the lipid molecule, respectively (Figure 1, framed middle panel). Because of this structure, lipids in aqueous solutions spontaneously form a *bilayer*, i.e., a sheetlike structure two molecules thick, with the nonpolar tails oriented inward and the polar heads pointing outward, contacting the water and dissolved ions surrounding the bilayer (Figure 1, right). The lipids are held together only by weak (noncovalent) interactions, and at sufficiently high temperatures, the bilayer behaves as a two-dimensional liquid, with the lipid molecules easily moving laterally within a specific layer of the bilayer, very rarely flipping into the other layer, and practically never spontaneously leaving the bilayer.

Despite the relative weakness of the pairwise interactions between the lipids, the cooperative nature of these interactions makes the lipid bilayer a very stable structure. Because of its nonpolar interior, it is also an almost impenetrable barrier for polar molecules dissolved in the aqueous electrolyte on both its sides. Nevertheless, water and some monoatomic ions permeate through it at rates too high to be explainable by diffusion through an entirely intact bilayer [9], [10]. Under certain conditions, e.g., sufficiently high temperature, surface tension, or both, this permeation can be attributed to the formation and rapid resealing of very small aqueous pores in the lipid bilayer, with radii below a nanometer and lifetimes below a nanosecond; they form and reseal because of thermal and mechanical fluctuations. This explanation is consistent with theory [11], [12], and has been corroborated by molecular dynamics (MD) simulations [13]–[15]. The pores can form without an external electric field acting on the membrane, but they are inherently unstable.

Enhancement of Pore Formation by Electric Fields—Electroporation

Exposure of biological membranes to a sufficiently high external electric field can lead to a rapid and large increase in their electric conductivity and permeability. This effect, generally referred to as *membrane electroporation* (or by some authors as *electropermeabilization*) and in food processing as *PEF treatment,* was reported for excitable biological cells in 1958 [1], for nonexcitable cells in 1967 [2], for lipid vesicles in 1972 [3], and for planar lipid bilayers in 1979 [16]. Considering that in all these cases the underlying physical mechanism is the same, it must take place in the lipid bilayer because it is the only molecular component common to all the membrane types. Pure lipid bilayers are therefore widely used as simple model systems for experimental investigations of membrane electroporation. There are two main approaches to such investigations, namely, the *voltage clamp* and the *current clamp*, based on applying voltage or current to the membrane and simultaneously measuring the voltage across the bilayer and the current flowing through it [17]. In our research, we typically use linearly increasing signals (either voltage or current) to determine the planar lipid bilayer breakdown voltage [18], as shown in Figure 2.

In many solid insulators, electrical breakdown causes permanent structural change and is generally irreversible. In contrast, the liquid-like behavior of the lipids allows the bilayer to return spontaneously to its prebreakdown state. If the exposure to the electric field is neither too long nor too intense, electroporation of the lipid bilayer is thus reversible. In the past, several theoretical descriptions of the events underlying electroporation have been proposed, based on assumptions of some form of elastic deformation [19]–[21], or on molecular-level events such as phase transitions [22], or on breakdown of

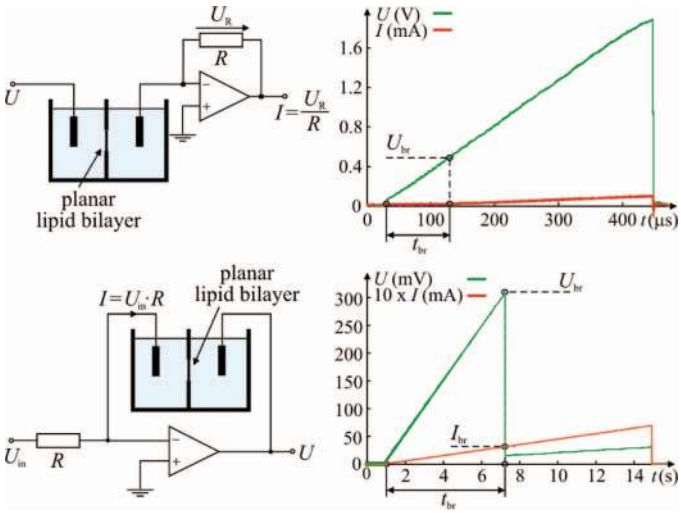

Figure 2. Typical circuits (left), and voltages and currents (U and I, right) measured in studying electroporation of a planar lipid bilayer. Top: the voltage clamp approach, in which voltage U is applied to the bilayer, and the current I through it is measured. Bottom: the current clamp approach, in which the input voltage U_{in} is transformed into current I and injected through the bilayer, and the voltage U across the bilayer is measured. The current clamp allows for a much slower increase in the voltage across the bilayer, and thus a more detailed monitoring of the breakdown. U_{br}, I_{br}, and t_{br} denote the breakdown voltage, current, and time, respectively. R is an ohmic resistor.

lipid domain interfaces [23]. However, each of these descriptions suffers from serious flaws [24]. Today, there is broad consensus that electroporation is best described by the theory of aqueous pore formation (hence the name). According to this theory [24], [25], the electrical field induces a voltage across the bilayer and reduces the energy required for spontaneous formation of aqueous pores in the bilayer (see the preceding subsection), thus facilitating the formation of a greater number of pores, and pores that are more stable, than in the absence of the electric field (Figure 3). Forming and stabilizing under the influence of the electric field, the pores have lifetimes ranging from milliseconds up to minutes after the field is removed. They then reseal, and are therefore categorized as *metastable*.

To date, all attempts to observe directly the pores formed in the lipid bilayer by electroporation have failed. With radii of at most several nanometers (see the plot in Figure 3), they are too small to be observed under an optical microscope, whereas sample preparation required for electron microscopy of soft matter (vacuumization, cryofixation or fixation by osmium tetroxide, metallic coating for scanning microscopy) is too aggressive and affects metastable structures in the bilayer. In fact, an early report of volcano-shaped electropores tens of nanometers in size [26] was later shown to be an artifact caused by sample preparation [27]. However, convincing corroboration of the theory of aqueous pore formation is now provided by MD simulations. As mentioned above, MD simulations provide some support for pore formation in the absence of an electric field. However, if in such simulations a sufficiently strong electric field is applied perpendicularly to the bilayer, the increase in the rate of pore formation, and pore stabilization based on the transition from the hydrophobic to the hydrophilic pore form (see Figures 3B and 3C), become clearly discernible [28], [29]. A molecular representation extracted from an MD simulation of lipid bilayer electroporation performed by our research groups is shown in Figure 4.

Theory, simulations, and experiments are in relatively good agreement regarding the qualitative properties of pore formation, (meta)stabilization, and resealing, but there are still some notable differences with respect to the quantitative description of these processes, particularly the dynamics of pore formation. Thus, MD simulations predict that, at transmembrane voltages of several hundred millivolts, pores in the lipid bilayer are formed within at most several nanoseconds [28]–[30], whereas

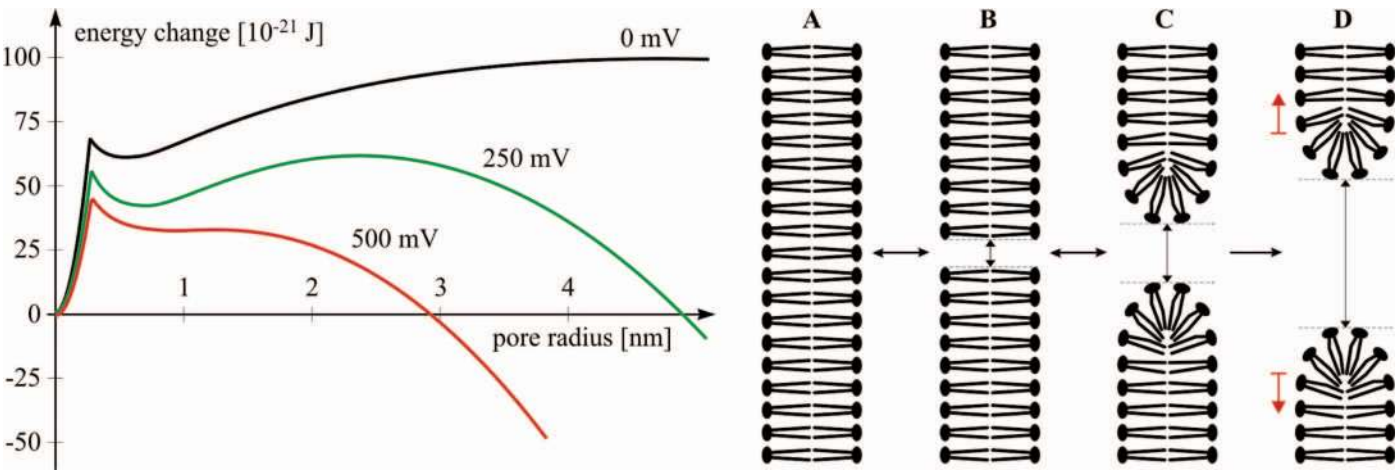

Figure 3. Left: change in lipid bilayer energy caused by formation of an aqueous pore, plotted as a function of the pore radius and voltage across the bilayer. Right: bilayer without pores (A), with a hydrophobic pore (B), its reversible transition into a metastable hydrophilic pore (C), and its irreversible transition into an unstable self-expanding hydrophilic pore (D; at membrane voltages above ~500 mV).

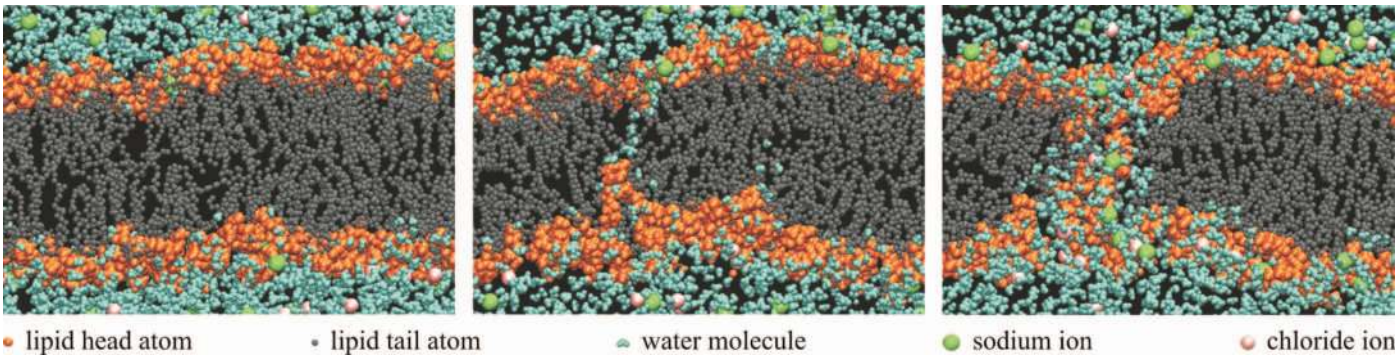

Figure 4. A molecular dynamics simulation of an aqueous pore forming in a lipid bilayer exposed to an electric field perpendicular to the bilayer plane. Left: the intact bilayer. Middle: water molecules penetrate the bilayer, forming a "water wire." Right: the adjacent lipids reorient with their heads toward the water molecules in the bilayer, stabilizing the aqueous pore and allowing the ions to enter.

experiments show a lag of several microseconds between the start of the pulse and the onset of detectable transmembrane transport. This lag is much longer than the time required for inducement of transmembrane voltage (see the next section) [31], [32]. This discrepancy implies that the details of pore formation or their subsequent (meta)stabilization, or both, are still not fully understood.

Biological Cell in an Electric Field

Induced Transmembrane Voltage

In typical experimental setups, the planar lipid bilayer is usually formed over a pinhole separating two compartments filled with an aqueous electrolyte solution. The bilayer is thus electrically connected in series between the two electrolytes, and the voltage across the bilayer is generated by immersing a pair of electrodes, one into each aqueous compartment (Figure 5A). Because the bilayer is much less electrically conductive than the electrolytes, the voltage across it is only slightly smaller than the voltage between the electrodes. Moreover, as long as the bilayer contains no pores, the voltage across it is the same everywhere, providing a controlled environment for studies of lipid bilayer electroporation (see the preceding section). In biological cells, an analogous setting can be achieved using two electrode-containing glass micropipettes, one forming a tight seal over a patch of the membrane, and the other rupturing the membrane at the opposite side of the cell (Figure 5B). Most of the voltage between the electrodes thus appear across the patch of the membrane, and the voltage across this patch is the same everywhere over the patch, allowing for controlled studies of cell membrane electroporation.

In many applications of electroporation, however, biological cells are generally not brought into direct contact with the electrodes (Figure 5C). Consequently, the voltage on the membranes of the exposed cells, termed the *induced transmembrane voltage* (*ITV*, denoted by $\Delta\Psi_m$), represents only a part of the voltage delivered to the electrodes. Moreover, unlike the voltage across planar bilayers and clamped membrane patches, the ITV is position dependent; thus in spherical cells, it varies proportionally to the cosine of the angle between the position on the membrane and the applied field direction, measured from the center of the cell (see below).

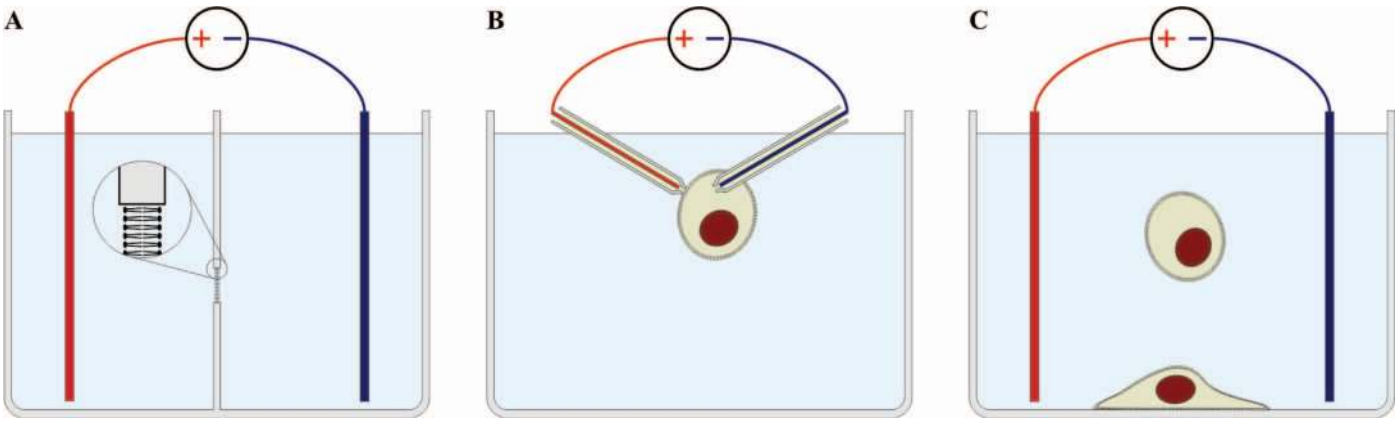

Figure 5. Exposure of membranes to electric fields: (A) a planar bilayer, (B) a membrane patch, (C) a cell suspended and a cell attached to a surface in an aqueous electrolyte.

Evaluation of Induced Voltage

For cells with sufficiently regular shapes (spheres, spheroids, cylinders) that are sufficiently far apart (in dilute suspensions), the time dependence and spatial distribution of the induced transmembrane voltage can be derived analytically. In the case of irregular shapes, or cells close to each other (in dense suspensions, cell clusters, tissues), or both, the analytical approach fails. However, when modern computers and numerical methods are used, the ITV induced on such cells can be evaluated sufficiently accurately. An alternative to both analytical and numerical determination of the ITV is the experimental approach based on potentiometric dyes. We now describe each of these approaches in more detail.

A) Analytical Derivation: The derivation of the ITV is based on solving the partial differential equation

$$\nabla\left[\left(\sigma + \varepsilon \tfrac{\partial}{\partial t}\right)\nabla\Psi(x,y,z,t)\right] = 0, \tag{1}$$

with σ denoting the electric conductivity, and ϵ denoting the dielectric permittivity of the point under consideration. In the steady state, the time derivatives are zero, and this equation simplifies into the Laplace equation

$$\nabla \cdot \nabla\Psi(x,y,z) = 0. \tag{2}$$

Solving this equation in a particular coordinate system and applying physically realistic boundary conditions (finiteness of Ψ, continuity of Ψ and its derivatives, asymptotic vanishing of the cell's effect on Ψ with increasing distance from the cell) yields the spatial distribution of Ψ. The induced transmembrane voltage is then calculated as the difference between the values of Ψ on both sides of the membrane:

$$\Delta\Psi_{\mathrm{m}} = \Psi_{\mathrm{int}} - \Psi_{\mathrm{ext}}. \tag{3}$$

For a single spherical cell with a nonconductive plasma membrane, the Laplace equation is solved in the spherical coordinate system, yielding the expression often referred to as the *steady-state Schwan equation* [33]:

$$\Delta\Psi_{\mathrm{m}} = \tfrac{3}{2}\, E\, R\, \cos\theta, \tag{4}$$

where R is the cell radius, E is the electric field, and θ is the angle measured from the center of the cell with respect to the direction of the field. Thus $\Delta\Psi_{\mathrm{m}}$ is proportional to the applied electric field and the cell radius, and it varies as $\cos\theta$, with extremal values at the points where the field is perpendicular to the membrane, i.e., at $\theta = 0°$ and $\theta = 180°$ (the "poles" of the cell).

The ITV as given by (4) is typically established within microseconds after the onset of the field. To describe the initial transient behavior, one uses the more general *first-order Schwan equation* [34]:

$$\Delta\Psi_{\mathrm{m}} = \tfrac{3}{2}\, E\, R\, \cos\theta\left[1 - \exp\left(-t/\tau_{\mathrm{m}}\right)\right], \tag{5a}$$

where τ_{m} is the time constant of membrane charging given by

$$\tau_{\mathrm{m}} = \frac{R\,\varepsilon_{\mathrm{m}}}{2d\dfrac{\sigma_{\mathrm{i}}\sigma_{\mathrm{e}}}{\sigma_{\mathrm{i}} + 2\sigma_{\mathrm{e}}} + R\,\sigma_{\mathrm{m}}}, \tag{5b}$$

with σ_{i}, σ_{m}, and σ_{e} denoting the conductivities of the cytoplasm, cell membrane, and extracellular medium respectively, ε_{m} denoting the dielectric permittivity of the membrane, and d denoting the membrane thickness.

In certain *in vitro* experiments, where artificial extracellular media with conductivities far below typical physiological values are used, the factor 3/2 in (4) and (5a) decreases, as described in detail in [34]. In general, (5a) is applicable to exposures to all rectangular electric pulses longer than 1 μs, as well as all sine (AC) electric fields with frequencies up to 1 MHz. To determine $\Delta\Psi_{\mathrm{m}}$ induced by shorter pulses or higher frequencies, the permittivities of the electrolytes surrounding the membrane also have to be taken into account, leading to further generalization of (5) to a second-order model [35]–[38].

Expressions similar to (4)–(5) can also be derived for nonspherical cells, provided they resemble a regular geometrical body such as a cylinder (e.g., muscle cells, axons of nerve cells), an oblate spheroid (e.g., erythrocytes), or a prolate spheroid (e.g., bacilli). To obtain the analogs of Schwan's equation for such cells, the Laplace equation is solved in a suitable coordinate system [39]–[41].

B) Numerical Computation: The ITV cannot be determined analytically for irregularly shaped cells or for cells in dense suspensions or in clusters, but it can be computed numerically, e.g., using the finite-differences or the finite-elements methods. The latter method is more suitable for irregularly shaped cells and clusters of such cells, and is generally implemented in four steps: 1) constructing a three-dimensional model of the cells of interest (e.g., from their cross-sectional images); 2) importing this model into a suitable numerical software package, thereby transforming the continuous geometry of the model into finite elements, and converting the partial differential equation (1) or (2) into a system of linear ordinary differential equations; 3) solving these equations numerically with suitable boundary conditions; 4) extracting the values of the electric potential on both sides of the membrane, and computing the ITV as their difference according to (3). This approach is summarized graphically in Figure 6.

To avoid explicit incorporation of the cell membrane, which because of its thinness would require the model to contain an extremely large number of finite elements, the membrane can be replaced by an interface with zero thickness and a suitable surface electric conductivity and surface dielectric permittivity [42], [43].

In addition to irregular cells, numerical computation can be used for determination of the ITV in cells in dense suspensions and in clusters. In dilute cell suspensions, the local field outside each cell is practically unaffected by other cells; for spherical cells, the deviation of ITV from the prediction given by (5a) is very small. However, for suspensions with cell volume fractions exceeding 10%, the ITV gradually begins to deviate from

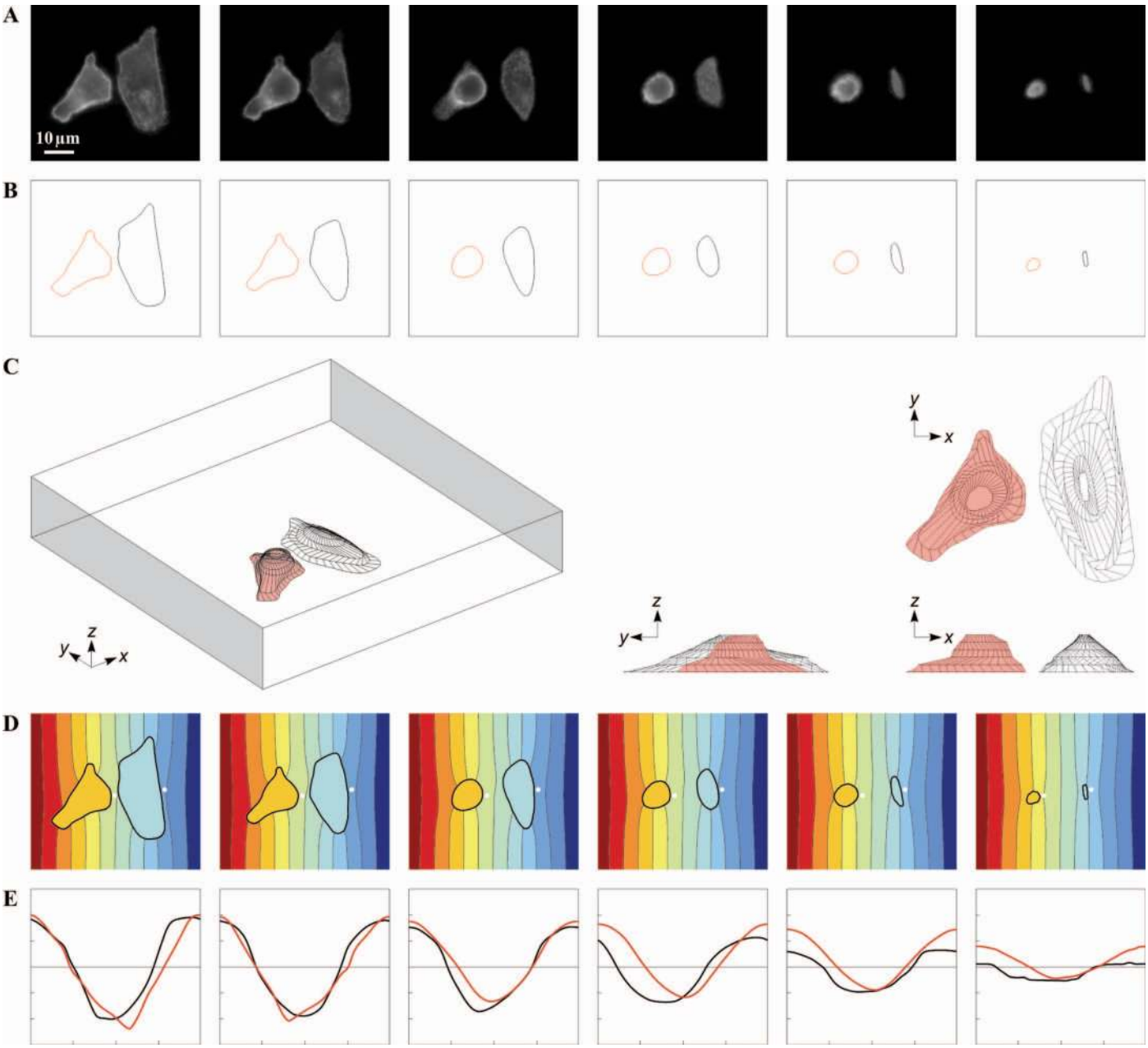

Figure 6. Numerical computation of the induced transmembrane voltage (ITV): (A) fluorescence cross-section images of two cells, (B) contours of their cross-sections, (C) three-dimensional model of the cells constructed from the contours, (D) computed distribution of electric potential, (E) computed ITV (red: left cell; black: right cell). Reprinted from [42] with permission.

(5a) and should be determined numerically using the methods described in the preceding two paragraphs [44]–[48].

C) Experimental Determination: An alternative to analytical derivation and numerical computation of the ITV is provided by experimental techniques. These include measurements with microelectrodes and with potentiometric fluorescent dyes. The invasive nature of microelectrodes, their low spatial resolution, and particularly their physical presence, which distorts the external electric field and hence the ITV that is being measured, are serious disadvantages. In contrast, measurements by means of potentiometric dyes are noninvasive (i.e., no physical disruption of the membrane occurs), they offer higher spatial resolution than microelectrodes, and their presence does not distort the electric field. As a consequence, potentiometric dyes, such as di-8-ANEPPS [49], [50], RH292 [31], and ANNINE-6 [51], have become established tools for measurements of ITV, experimental studies of voltage-gated membrane channels, and monitoring of nerve and muscle cell activity. These dyes are incorporated into the lipid bilayer of the cell plasma membrane, where they start to fluoresce, with their fluorescence spectra being dependent on the amplitude of the ITV (Figure 7A). With a suitable experimental setup incorporating a pulse laser, a fast and sensitive camera, and a system for synchronizing the acquisition with the field exposure, these dyes enable monitoring of the time variation

of ITV with a resolution of microseconds, and in the case of ANNINE-6, down to nanoseconds.

Monitoring of Electroporation

As described in the Electroporation subsection of the Lipid Bilayer in an Electric Field section, the pores in the membrane caused by electroporation have not yet been observed directly. As a consequence, electroporation has to be detected and studied by assessing its larger scale manifestations, such as the changes in the electrical or optical properties of the membrane resulting from pore formation, or transport through the pores. The changes in the electrical properties of the membrane can be measured by forming a direct contact between a patch of the membrane and an electrode-containing micropipette, using a setup resembling that shown in Figure 5B. During electroporation the conductance of the membrane patch increases by several orders of magnitude, and the capacitance is also altered measurably [52]–[54].

In a sufficiently dense cell suspension, electroporation can also be monitored by measuring the bulk electric conductivity of the suspension, which increases significantly if a large fraction of the suspended cells is electroporated [55], [56]. In tissues, electroporation also affects the frequency dependence of their bulk electric conductivity and dielectric permittivity, and can thus be assessed by measuring the impedance spectrum of the tissue before and after exposure to electric pulses (and possibly also between consecutive pulses). However, the rapid resealing of electroporated membranes prohibits a detailed frequency sweep; thus in practice, only one point or a few points of the spectrum are measured, typically in the kilohertz range. Successful implementation of this approach has been reported, e.g., for skin [57] and liver [58], allowing for a distinction between nonporated, reversibly porated, and irreversibly porated tissues.

The bulk optical properties of the membrane, particularly light scattering and absorption, are also affected by the reorientation of lipids around the pores, and measurements of these properties can also be used to assess electroporation [59]. Finally, an even more indirect method (and also the most frequently used) is through imaging of the transport of molecules that cannot permeate an intact membrane. This approach is described in more detail below.

Transport Across the Electroporated Membrane

Transmembrane Voltage and Transport

In theory, a high absolute value of the ITV reduces the energy required for pore formation (see Figure 3), so one would expect the majority of the pores formed in the membrane to be located in the regions with the highest ITV. For isolated cells, both suspended and attached, and irrespective of cell shape, observations using fluorescence microscopy corroborate this theoretical prediction [31], [60]. The correlation between the ITV and the electroporation-mediated transport across the membrane can be demonstrated particularly clearly by combining potentiometric measurements and monitoring of transmembrane transport on the same cell [61]. An example is shown in Figure 7. For cells in clusters and tissues, the correlation between the ITV and the transport regions is more difficult to demonstrate directly because of the presence of intracellular pathways (some of them voltage sensitive) and

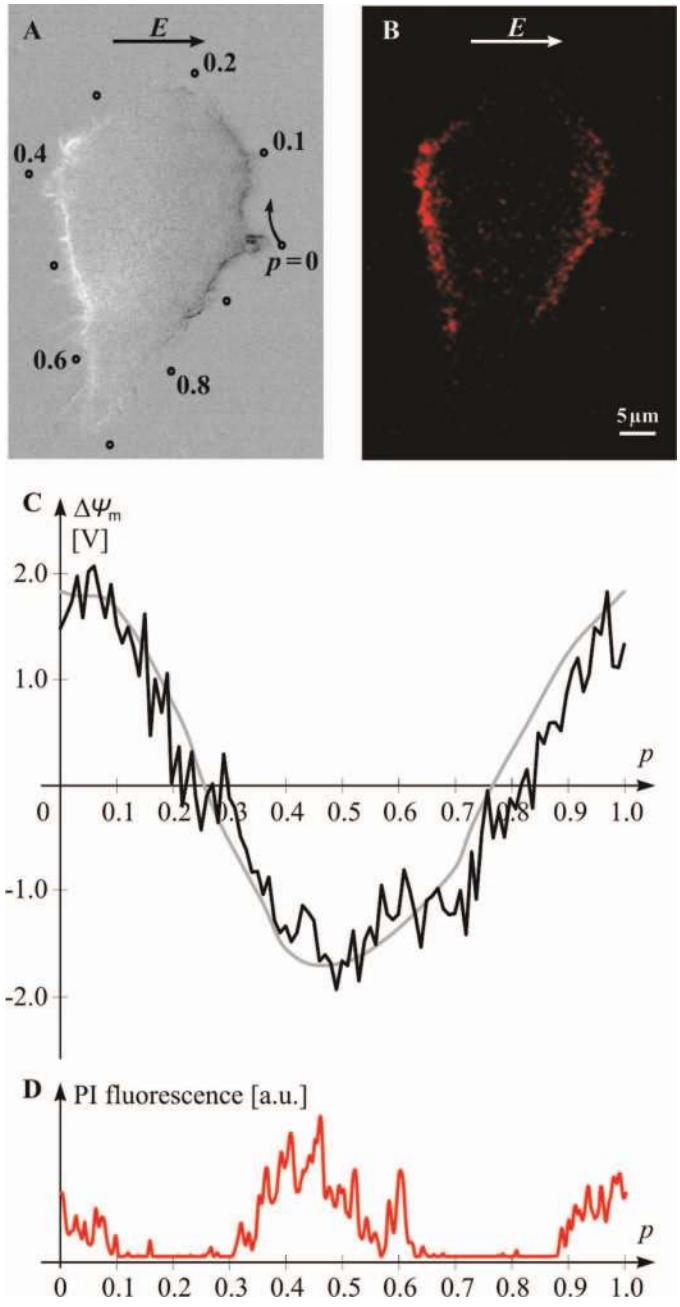

Figure 7. The induced transmembrane voltage (ITV) and electroporation of an irregularly shaped Chinese-hamster-ovary (CHO) cell: (A) changes in fluorescence of di-8-ANEPPS reflecting the ITV, with dark regions corresponding to membrane depolarization and bright regions corresponding to membrane hyperpolarization; (B) fluorescence of propidium iodide (PI), reflecting transport of PI across the membrane; (C) ITV along the path shown in (A) as measured (black) and as predicted by numerical computation (gray); (D) fluorescence of PI along the path shown in (A). Adapted from [61] with permission.

nonuniform penetration of the dyes. On a more macroscopic level of a tissue, the correlation between the ITV and electroporation-mediated transport across the membrane is reflected in the fact that the tissue regions with the highest local electric field are generally also the regions containing the highest fractions of electroporated cells [62].

Electrophoretic and Diffusive Transport

The transport of molecules across an electroporated membrane can be characterized by the Nernst-Planck equation:

$$\frac{V}{S_{\mathrm{P}}}\frac{\mathrm{d}c}{\mathrm{d}t} = -D\frac{z\,E\,F}{\rho\,T}c - D\,\nabla c, \tag{6}$$

where V is the volume of the cell, S_{p} is the surface area of the electroporated part of the membrane, c the concentration of the molecules or ions transported across this part of the membrane, D is the diffusion coefficient for such transport, z the electric charge of the molecules or ions, E is the local electric field acting on them, F is the Faraday constant, ρ is the gas constant, and T is the absolute temperature. The first term on the right represents electrophoretic transport driven by the exposure of the cell to the electric field, and the second term represents diffusive transport that persists until either the concentrations of the transported molecules on both sides of the membrane equalize, or the cell membrane recovers from electroporation, i.e., until all the pores reseal. During the electric pulse(s), the electric field is the main source of the driving force acting on charged molecules and ions, and the electrophoretic term dominates the right-hand side of (6). After the end of the pulse, the electrophoretic transport ceases, with only the diffusive component persisting. Although the latter proceeds at a considerably slower rate, the membrane recovery time after electroporation is several orders of magnitude longer than the pulse duration used for electroporation (seconds to minutes, compared with microseconds to milliseconds). Consequently, despite the fast initial rate of electrophoretic transport, the total transport of both ions and small molecules through an electroporated membrane is often predominantly diffusive [63], [64]. In contrast, for macromolecules, particularly DNA, electrophoresis can play a vital role in the electroporation-facilitated transport across the membrane [65], [66].

Dynamics of Pore Resealing

Reversible electroporation requires sufficiently rapid membrane recovery so that the cell remains viable. When monitoring the transport across an electroporated membrane, such a recovery is reflected in the transport rate decreasing more rapidly than the theoretical prediction given by (6) under the assumption of constant S_{p} and D. Accurate measurements of the transport rate thus allow for estimation of the rate of decrease of S_{p} and D to zero, and thus of the time dependence of membrane recovery (D can be transferred from the right-hand side of (6) into the denominator of the fraction V/S_{p} on the left-hand side, so it is not important whether we model the decrease to zero of S_{p}, D, or their product). Such measurements show that the membrane recovery (or, microscopically, pore resealing) consists of several stages. Various studies disagree on matters of detail, but generally there is agreement that a very rapid phase (occurring in microseconds after the end of the pulse) is followed by several slower phases lasting from milliseconds to tens of seconds, or even minutes [31], [32], [67], [68].

Conclusions

In this article, the first in a series of three focusing on cell membrane electroporation, we discussed the phenomenon itself, describing aqueous pore formation on the submicroscopic level of the lipid molecules forming the membrane, and on the microscopic level of individual biological cells enveloped by such a membrane. We also described molecular transport through the electroporated membrane, which is the basis of various applications of electroporation in medicine and biotechnology. The second article will be devoted to these applications, specifically electroporation on the larger scale level of tissues, the basis of several efficient treatments in medicine and promising techniques in biotechnology. The third article will focus on the equipment required for electroporation.

Acknowledgments

This work was in part supported by the Slovenian Research Agency under various grants. Research was conducted within the scope of the Pulsed Electric Field Applications in Biology and Medicine (EBAM) European Associated Laboratory (LEA). This manuscript is a result of the networking efforts of the European Cooperation in Science and Technology (COST) Action TD1104.

References

[1] R. Stämpfli, "Reversible electrical breakdown of the excitable membrane of a Ranvier node," *An. Acad. Brasil. Ciens.*, vol. 30, pp. 57–63, 1958.

[2] A. J. H. Sale and W. A. Hamilton, "Effects of high electric fields on microorganisms: I. Killing of bacteria and yeasts," *Biochim. Biophys. Acta*, vol. 148, pp. 781–788, 1967.

[3] E. Neumann and K. Rosenheck, "Permeability changes induced by electric impulses in vesicular membranes," *J. Membrane Biol.*, vol. 10, pp. 279–290, 1972.

[4] G. Serša, D. Miklavčič, M. Čemažar, Z. Rudolf, G. Pucihar, and M. Snoj, "Electrochemotherapy in treatment of tumours," *Eur. J. Surg. Oncol.*, vol. 34, pp. 232–240, 2008.

[5] F. André and L. M. Mir, "DNA electrotransfer: Its principles and an updated review of its therapeutic applications," *Gene Ther.*, vol. 11, pp. S33–S42, 2004.

[6] E. W. Lee, S. Thai, and S. T. Kee, "Irreversible electroporation: A novel image-guided cancer therapy," *Gut Liver*, vol. 4, pp. S99–S104, 2010.

[7] M. Sack, J. Sigler, S. Frenzel, C. Eing, J. Arnold, T. Michelberger, W. Frey, F. Attmann, L. Stukenbrock, and G. Müller, "Research on industrial-scale electroporation devices fostering the extraction of substances from biological tissue," *Food Eng. Rev.*, vol. 2, pp. 147–156, 2010.

[8] M. Morales-de la Peña, P. Elez-Martínez, and O. Martín-Belloso, "Food preservation by pulsed electric fields: An engineering perspective," *Food Eng. Rev.*, vol. 3, pp. 94–107, 2011.

[9] D. W. Deamer and J. Bramhall, "Permeability of lipid bilayers to water and ionic solutes," *Chem. Phys. Lipids*, vol. 40, pp. 167–188, 1986.

[10] M. Jansen and A. Blume, "A comparative study of diffusive and osmotic water permeation across bilayers composed of phospholipids with different headgroups and fatty acyl chains," *Biophys. J.*, vol. 68, pp. 997–1008, 1995.

[11] J. D. Litster, "Stability of lipid bilayers and red blood cell membranes," *Phys. Lett.*, vol. 53A, pp. 193–194, 1975.

[12] R. Lawaczeck, "Defect structures in membranes: Routes for the permeation of small molecules," *Ber. Bunsenges. Phys. Chem.*, vol. 92, pp. 961–963, 1988.

[13] J. C. Shillcock and U. Seifert, "Thermally induced proliferation of pores in a model fluid membrane," *Biophys. J.*, vol. 74, pp. 1754–1766, 1998.
[14] H. Leontiadou, A. E. Mark, and S. J. Marrink, "Molecular dynamics simulations of hydrophilic pores in lipid bilayers," *Biophys. J.*, vol. 86, pp. 2156–2164, 2004.
[15] A. A. Gurtovenko, J. Anwar, and I. Vattulainen, "Defect-mediated trafficking across cell membranes," *Chem. Rev.*, vol. 110, pp. 6077–6103, 2010.
[16] R. Benz, F. Beckers, and U. Zimmermann, "Reversible electrical breakdown of lipid bilayer membranes: A charge-pulse relaxation study," *J. Membrane Biol.*, vol. 48, pp. 181–204, 1979.
[17] P. Kramar, D. Miklavčič, M. Kotulska, and A. Maček Lebar, "Voltage- and current-clamp methods for determination of planar lipid bilayer properties," in *Advances in Planar Lipid Bilayers and Liposomes*, vol. 11, A. Iglič, Ed., Amsterdam, Elsevier, 2010, pp. 29–69.
[18] P. Kramar, D. Miklavčič, and A. Maček Lebar. "Determination of the lipid bilayer breakdown voltage by means of a linear rising signal," *Bioelectrochemistry,* vol. 70, pp. 23–27, 2007.
[19] D. H. Michael and M. E. O'Neill, "Electrohydrodynamic instability in plane layers of fluid," *J. Fluid Mech.*, vol. 41, pp. 571–580, 1970.
[20] J. M. Crowley, "Electrical breakdown of bimolecular lipid membranes as an electro-mechanical instability," *Biophys. J.*, vol. 12, pp. 711–724, 1973.
[21] A. Steinchen, D. Gallez, and A. Sanfeld, "A viscoelastic approach to the hydrodynamic stability of membranes," *J. Colloid Interface Sci.*, vol. 85, pp. 5–15, 1982.
[22] I. P. Sugar, "A theory of the electric field-induced phase transition of phospholipid bilayers," *Biochim. Biophys. Acta*, vol. 556, pp. 72–85, 1979.
[23] L. Cruzeiro-Hansson and O. G. Mouritsen, "Passive ion permeability of lipid membranes modelled via lipid-domain interfacial area," *Biochim. Biophys. Acta*, vol. 48, pp. 181–204, 1979.
[24] J. C. Weaver and Y. A. Chizmadzhev, "Theory of electroporation: A review," *Bioelectrochem. Bioenerg.*, vol. 41, pp. 135–160, 1996.
[25] R. W. Glaser, S. L. Leikin, L. V. Chernomordik, V. F. Pastushenko, and A. I. Sokirko, "Reversible electrical breakdown of lipid bilayers: Formation and evolution of pores," *Biochim. Biophys. Acta*, vol. 940, pp. 275–287, 1988.
[26] D. C. Chang and T. S. Reese, "Changes of membrane structure induced by electroporation as revealed by rapid-freezing electron microscopy," *Biophys. J.*, vol. 58, pp. 1–12, 1990.
[27] E. P. Spugnini, G. Arancia, A. Porrello, M. Colone, G. Formisano, A. Stringaro, G. Citro, and A. Molinari, "Ultrastructural modifications of cell membranes induced by electroporation on melanoma xenografts," *Microsc. Res. Tech.*, vol. 70, pp. 1041–1050, 2007.
[28] D. P. Tieleman, H. Leontiadou, A. E. Mark, and S. J. Marrink, "Simulation of pore formation in lipid bilayers by mechanical stress and electric fields," *J. Am. Chem. Soc.*, vol. 125, pp. 6282–6383, 2003.
[29] M. Tarek, "Membrane electroporation: A molecular dynamics simulation," *Biophys. J.*, vol. 88, pp. 4045–4053, 2005.
[30] R. A. Böckmann, B. L. De Groot, S. Kakorin, E. Neumann, and H. Grubmüller," Kinetics, statistics, and energetics of lipid membrane electroporation studied by molecular dynamics simulations," *Biophys. J.*, vol. 95, pp. 1837–1850, 2008.
[31] M. Hibino, H. Itoh, and K. Kinosita, Jr., "Time courses of cell electroporation as revealed by submicrosecond imaging of transmembrane potential," *Biophys. J.*, vol. 64, pp. 1789–1800, 1993.
[32] G. Pucihar, T. Kotnik, D. Miklavčič, and J. Teissié, "Kinetics of transmembrane transport of small molecules into electropermeabilized cells," *Biophys. J.*, vol. 95, pp. 2837–2848, 2008.
[33] H. Pauly and H. P. Schwan, "Über die Impedanz einer Suspension von kugelformigen Teilchen mit einer Schale," *Z. Naturforsch. B*, vol. 14, pp. 125–131, 1959.
[34] T. Kotnik, F. Bobanović, and D. Miklavčič, "Sensitivity of transmembrane voltage induced by applied electric fields—A theoretical analysis," *Bioelectrochem. Bioenerg.*, vol. 43, pp. 285–291, 1997.
[35] C. Grosse and H. P. Schwan, "Cellular membrane potentials induced by alternating fields," *Biophys. J.*, vol. 63, pp. 1632–1642, 1992.
[36] T. Kotnik, D. Miklavčič, and T. Slivnik, "Time course of transmembrane voltage induced by time-varying electric fields—A method for theoretical analysis and its application," *Bioelectrochem. Bioenerg.*, vol. 45, pp. 3–16, 1998.
[37] T. Kotnik and D. Miklavčič, "Second-order model of membrane electric field induced by alternating external electric fields," *IEEE Trans. Biomed. Eng.*, vol. 47, pp. 1074–1081, 2000.
[38] T. Kotnik and D. Miklavčič, "Theoretical evaluation of voltage inducement on internal membranes of biological cells exposed to electric fields," *Biophys. J.*, vol. 90, pp. 480–491, 2006.
[39] J. Bernhard and H. Pauly, "Generation of potential differences across membranes of ellipsoidal cells in an alternating electrical field," *Biophysik*, vol. 10, pp. 89–98, 1973.
[40] T. Kotnik and D. Miklavčič, "Analytical description of transmembrane voltage induced by electric fields on spheroidal cells," *Biophys. J.*, vol. 79; pp. 670–679, 2000.
[41] J. Gimsa and D. Wachner, "Analytical description of the transmembrane voltage induced on arbitrarily oriented ellipsoidal and cylindrical cells," *Biophys. J.*, vol. 81, pp. 1888–1896, 2001.
[42] G. Pucihar, T. Kotnik, B. Valič, and D. Miklavčič, "Numerical determination of transmembrane voltage induced on irregularly shaped cells," *Annals Biomed. Eng.*, vol. 34, pp. 642–652, 2006.
[43] G. Pucihar, D. Miklavčič, and T. Kotnik, "A time-dependent numerical model of transmembrane voltage inducement and electroporation of irregularly shaped cells," *IEEE Trans. Biomed. Eng.*, vol. 56, pp. 1491–1501, 2009.
[44] R. Susil, D. Šemrov, and D. Miklavčič, "Electric field induced transmembrane potential depends on cell density and organization," *Electro. Magnetobiol.*, vol. 17, pp. 391–399, 1998.
[45] M. Pavlin, N. Pavšelj, and D. Miklavčič, "Dependence of induced transmembrane potential on cell density, arrangement, and cell position inside a cell system," *IEEE Trans. Biomed. Eng.*, vol. 49, pp. 605–612, 2002.
[46] T. Heida, J. B. M. Wagenaar, W. L. C. Rutten, and E. Marani, "Investigating membrane breakdown of neuronal cells exposed to nonuniform electric fields by finite-element modeling and experiments," *IEEE Trans. Biomed. Eng.*, vol. 49, pp. 1195–1203, 2002.
[47] G. Pucihar, T. Kotnik, J. Teissié, and D. Miklavčič, "Electroporation of dense cell suspensions," *Eur. Biophys. J.*, vol. 36, pp. 173–185, 2007.
[48] W. Ying and C. S. Henriquez, "Hybrid finite element method for describing the electrical response of biological cells to applied fields," *IEEE Trans. Biomed. Eng.*, vol. 54, pp. 611–620, 2007.
[49] D. Gross, L. M. Loew, and W. Webb, "Optical imaging of cell membrane potential changes induced by applied electric fields," *Biophys. J.*, vol. 50, pp. 339–348, 1986.
[50] G. Pucihar, T. Kotnik, and D. Miklavčič, "Measuring the induced membrane voltage with di-8-ANEPPS," *J. Vis. Exp.*, vol. 33, p. 1659, 2009.
[51] W. Frey, J. A. White, R. O. Price, P. F. Blackmore, R. P. Joshi, R. L. Nuccitelli, S. J. Beebe, K. H. Schoenbach, and J. F. Kolb, "Plasma membrane voltage changes during nanosecond pulsed electric field exposure," *Biophys. J.*, vol. 90, pp. 3608–3615, 2006.
[52] R. Benz and F. Conti, "Reversible electrical breakdown of squid gian axon membrane," *Biochim. Biophys. Acta*, vol. 645, pp. 115–123, 1981.
[53] F. Rytssen, C. Farre, C. Brennan, S. G. Weber, K. Nolkrantz, K. Jardemark, D. T. Chiu, and O. Orwar, "Characterization of single-cell electroporation by using patch-clamp and fluorescence microscopy," *Biophys. J.*, vol. 79, pp. 1993–2001, 2000.
[54] A. G. Pakhomov, J. F. Kolb, J. A. White, R. P. Joshi, S. Xiao, and K. H. Schoenbach, "Long-lasting plasma membrane permeabilization in mammalian cells by nanosecond pulsed electric field (nsPEF)," *Bielectromagnetics*, vol. 28, pp. 655–663, 2007.
[55] K. Kinosita, Jr. and T. Y. Tsong, "Voltage-induced conductance in human erythrocyte membranes," *Biochim. Biophys. Acta*, vol. 554, pp. 479–497, 1979.
[56] M. Pavlin, V. Leben, and D. Miklavčič, "Electroporation in dense cell suspensions—Theoretical and experimental analysis of ion diffusion and cell permeabilization," *Biochim. Biophys. Acta*, vol. 1770, pp. 12–23, 2007.
[57] U. Pliquett and M. R. Prausnitz, "Electrical impedance spectroscopy for rapid and noninvasive analysis of skin electroporation," *Meth. Mol. Med.*, vol. 37, pp. 377–406, 2000.

[58] A. Ivorra and B. Rubinsky, "*In vivo* electrical impedance measurements during and after electroporation of rat liver," *Bioelectrochemistry*, vol. 70, pp. 287–295, 2007.
[59] S. Kakorin, S. P. Stoylov, and E. Neumann, "Electro-optics of membrane electroporation in diphenylhexatriene-doped lipid bilayer vesicles," *Biophys. Chem.*, vol. 58, pp. 109–116, 1996.
[60] B. Gabriel and J. Teissié, "Time courses of mammalian cell electropermeabilization observed by millisecond imaging of membrane property changes during the pulse," *Biophys. J.*, vol. 76, pp. 2158–2165, 1999.
[61] T. Kotnik, G. Pucihar, and D. Miklavčič, "Induced transmembrane voltage and its correlation with electroporation-mediated molecular transport," *J. Membrane Biol.*, vol. 236, pp. 3–13, 2010.
[62] D. Miklavčič, D. Šemrov, H. Mekid, and L. M. Mir, "A validated model of in vivo electric field distribution in tissues for electrochemotherapy and for DNA electrotransfer for gene therapy," *Biochim. Biophys. Acta*, vol. 1532, pp. 73–83, 2000.
[63] M. P. Rols and J. Teissié, "Electropermeabilization of mammalian cells: Quantitative analysis of the phenomenon," *Biophys. J.*, vol. 58, pp. 1089–1098, 1990.
[64] M. Puc, T. Kotnik, L. M. Mir, and D. Miklavčič, "Quantitative model of small molecules uptake after in vitro cell electropermeabilization," *Bioelectrochemistry*, vol. 60, pp. 1–10, 2003.
[65] M. Pavlin, K. Flisar, and M. Kandušer, "The role of electrophoresis in gene electrotransfer," *J. Membrane Biol.*, vol. 236, pp. 75–79, 2010.
[66] J. M. Escoffre, T. Portet, C. Favard, J. Teissié, D. S. Dean, and M. P. Rols, "Electromediated formation of DNA complexes with cell membranes and its consequences for gene delivery," *Biochim. Biophys. Acta*, vol. 1808, pp. 1538–1543, 2011.
[67] M. P. Rols, F. Dahhou, K. P. Mishra, and J. Teissié, "Control of electric-field induced cell membrane permeabilization by membrane order," *Biochemistry*, vol. 29, pp. 2960–2966, 1990.
[68] E. Neumann, K. Toensing, S. Kakorin, P. Budde, and J. Frey, "Mechanism of electroporative dye uptake by mouse B cells," *Biophys. J.*, vol. 74, pp. 98–108, 1998.

Tadej Kotnik was born in 1972. He received a Ph.D. in biophysics from the University of Paris XI, France, and a Ph.D. in electrical engineering from the University of Ljubljana, Slovenia, both in 2000. He is currently an associate professor in the Faculty of Electrical Engineering at the University of Ljubljana. His research interests include membrane electrodynamics, theoretical and experimental study of related biophysical phenomena, particularly membrane electroporation, and computational research in number theory. In 2001 he received the Galvani Prize of the Bioelectrochemical Society.

Peter Kramar was born in 1977. He received a Ph.D. in electrical engineering from the University of Ljubljana, Slovenia, in 2010. He is currently a teaching assistant in the Faculty of Electrical Engineering at the University of Ljubljana. His current research interests include electroporation of planar lipid bilayers.

Gorazd Pucihar was born in 1976. He received a Ph.D. in electrical engineering from the University of Ljubljana, Slovenia, and University of Toulouse III–Paul Sabatier, France, in 2006. He is currently an assistant professor in the Faculty of Electrical Engineering at the University of Ljubljana. His research work is focused on experimental investigation and numerical modeling of electroporation and related phenomena.

Damijan Miklavčič was born in 1963. He received a Ph.D. in electrical engineering from the University of Ljubljana, Slovenia, in 1993. He is currently a full professor, head of the Laboratory of Biocybernetics, and head of the Department of Biomedical Engineering in the Faculty of Electrical Engineering at the University of Ljubljana. For the last few years his research has been focused on electroporation-based gene transfer and drug delivery, development of electronic hardware, and numerical modeling of biological processes.

Mounir Tarek was born in 1964. He received a Ph.D. in physics from the University of Paris, France, in 1994. He is currently a senior research scientist (Directeur de Recherches) of the CNRS at the University of Nancy–Henri Poincaré, France. He joined the CNRS after 3 years as a postdoctoral scientist at the University of Pennsylvania, and a 4-year tenure at the National Institute of Standards and Technology, Gaithersburg, Maryland. During the last few years, he has worked on large-scale, state-of-the-art molecular simulations of lipid membranes and transmembrane proteins, probing their structure and dynamics.